Indian Journal of Pure & Applied Physics
Vol. 59, September 2021, pp. 638-642

Structural and Magnetic Properties of Ce/Fe Doped $YCrO_3$ Ceramic

Liran Shi*, Jian Li, Jin Wang & Xiangming Chen

School of Physics and Electrical Engineering, AnYang Normal University, Henan Anyang, 455000 China

Received 15 January 2021; accepted 11 August 2021

The structure and magnetic properties of perovskite chromium oxide YCrO3 and its doping system are systematically studied. Ceramic samples are prepared by solid state method. X-ray diffraction patterns reveal that the materials are orthorhombic structure with space group Pnma. The result of magnetic study of YCrO3 and the doping system show that the antiferromagnetism and ferromagnetism coexist in the system. The magnetism comes from the exchange interactions between Cr ions. The results of magnetothermal curve reveal that all the samples show the negative magnetization induced by temperature and doping at different positions affects the compensation temperature, which is related to the interaction of magnetic ions in the system. The doping of Ce ions in Y-position affects the coercivity of hysteresis loop, but it has no effect on the magnitude of magnetization. While, the doping of Fe ions enhances the antiferromagnetism of the system and makes the magnetization decrease obviously. The phenomenon of negative magnetization in the sample makes it possible for this kind of material to be used in magnetic sensor parts.

Keywords: Chromic acid yttrium, Negative magnetization, Canted antiferromagnetism, Ferromagnetism

1 Introduction

The oxide RMO_3 (R = rare earth ions or yttrium, M = 3*d*, 4*d* transition metal) with perovskite structure have attracted considerable attention in recent years, due to its simple structure, rich magnetism, electrical properties, high temperature superconductivity, giant magnetoresistance effect and multiferroicity[1-4]. Magnetization reversal or negative magnetization in the $RCrO_3$ materials has been well known in recent years[5-9]. It exhibits a net zero magnetization at a characteristic temperature named as compensation temperature (T_{comp}). Rare-earth chromate $RCrO_3$ with orthogonally distorted perovskite structure, each cell containing four molecules, belongs to *Pnma* space group. The system has complex magnetic characteristics because of the interaction between transition metal ions and rare earth ions, which has attracted extensive attention and in-depth research. The spin magnetic order of the 3*d* electron of Cr^{3+} and the 4*f* electron of R^{3+} play an important role in the magnetoelectric coupling of the $RCrO_3$ system[10]. At low temperatures, there are *d-d* interactions between transition metals, *f-f* interactions between rare earth ions, and *f-d* interactions between rare earth ions and transition metals. The spin of Cr^{3+} produces a spontaneous antiferromagnetic order at the Neel temperature T_N. The bond angle of Cr^{3+}-O^{2-}-Cr^{3+}deviates 180° due to the competition between single ion anisotropy and the antisymmetric Dzyaloshinsky–Moriya (DM) interaction, the spin of Cr^{3+} is canted antiferromagnetism, and the system shows weak ferromagnetism. The magnetization reversal phenomenon is previously observed in $GdCrO_3$[11], $La_{1-x}Pr_xCrO_3$[12], $YFe_{1-x}Mn_xO_3$[13], $BiFe_{0.5}Mn_{0.5}O_3$[14] and some other perovskites. There are different explanations for the origin of negative magnetization in different systems. Magnetization inversion in orthogonal chromium oxides is caused by the antiferromagnetic coupling between rare earth and transition metal ions[11,12], while in $YFe_{1-x}Mn_xO_3$ and $BiFe_{0.5}Mn_{0.5}O_3$, the random occupation of magnetic ions at the B-site in the perovskite structure has been suggested to be responsible for the magnetization reversal[15-17]. In the orthovanadates, the competition between single-ion magnetic anisotropy and antisymmetric Dzyaloshinsky-Moriya (DM) interaction is considered to be the origin of negative magnetization.

Based on the physical mechanism of magnetization reversal mentioned above, the Y-site and Cr-site sublattices are simultaneously involved in the process of magnetization reversal. The cationic substitution of the Y and Cr positions in the perovskite structure has been shown to be an effective substitute for inducing new phenomena or improving magnetic and transport properties[18-22]. Sinha *et al.*[23] reported that the enhanced relaxer ferroelectric behavior has been observed with the increasing Nd doping in $YCrO_3$. The effect of Eu, Sm and Er doping in $YCrO_3$ on the

*Corresponding author: (E-mail: shiliran1127@126.com)

electrical and magnetic properties was reported by Chakraborty *et al.*[24-26]. The decrease of T_N, coercive field and magnetization value with the increase of Al concentration in $YCrO_3$ was observed, and two mechanisms that tune the magnetic properties were discussed and proposed[27]. The detail magnetic behavior of Mn doped $YCrO_3$ was studied by Hashimi *et al.*[28] and by Wang *et al.*[29]. The R-Cr interaction in response to magnetic field and temperature is argued to be the major factor for the intriguing properties of these compounds[30,31]. The fundamental importance of doping in enhancing the electrical and magnetic properties which will open up the possibility of $YCrO_3$ to be used in spintronic. Therefore, considering the importance of $YCrO_3$, the Ce doping and Fe doping effect on the magnetic properties is systematically investigated in this paper.

2 Experiment

Polycrystalline samples were prepared by solid state reaction method with the stoichiometric quantities of Y_2O_3 (99.9%), Cr_2O_3 (99.9%), Fe_2O_3 (99.9%) and CeO_2 (99.9%) as starting materials. The mixture was sintered at 900 °C for 12 h after fully grinding, and then 1200 °C for 12 h. After that, the powder products were reground and pressed into pellets with 13 mm diameter and 1 mm thickness. The pressure for making $YCrO_3$ ceramic pellets was 12 Mpa and the time was 5 min. Finally, the pellets were sintered at 1450 °C for 48 h.

Phase purity of all prepared samples was confirmed by a powder X-ray diffractometer (XRD, Burker AXS) with Cu-Kα radiation. Morphology studies and composition analysis have been carried using field emission scanning electron microscope (FE-SEM) instrument. The magnetic properties were measured using a vibrating sample magnetometer Versalab-VSM (Quantum Design). Zero field cooling (ZFC) and field cooling (FC) models were used to measure the variation curve of magnetization with temperature from 50 K to 350 K. Hysteresis loops were measured with the magnetic field from -3 T to 3T.

Result and discussion

Fig. 1 shows the room temperature X-ray diffraction patterns of (a)$YCrO_3$, (b) $Y0.9Ce_{0.1}CrO_3$ and (c) $YCr_{0.9}Fe_{0.1}O_3$. The results showed that all the diffraction peaks can be assigned to the single phase orthorhombic structure with space group Pnma. No other impurity peaks were found, and the samples had good monophasic properties. The composition of the synthesized samples is verified by energy-dispersive analysis of X-ray (EDAX) technique and the spectrum is shown in Fig. 2. The results showed that the compositions of the samples are retained and showed peaks according to their concentrations. There is no loss of integral elements in the samples. The insets of

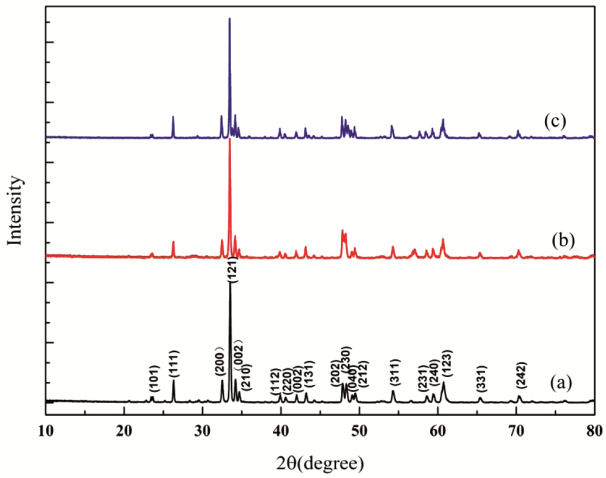

Fig. 1 — The room temperature XRD patterns for polycrystalline compounds (a) $YCrO_3$, (b) $Y_{0.9}Ce_{0.1}CrO_3$ and (c) $YCr_{0.9}Fe_{0.1}O_3$.

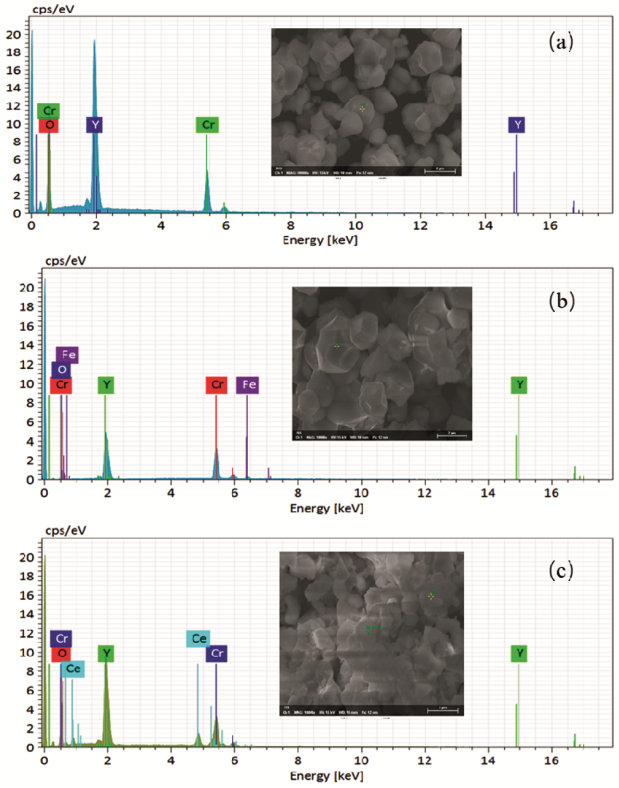

Fig. 2 — EDX patterns of (a) $YCrO_3$, (b) $YCr_{0.9}Fe_{0.1}O_3$ and (c) $Y_{0.9}Ce_{0.1}CrO_3$. The micrographs of samples are shown in the insets.

Fig. 2 display the surface morphology of the samples. Clear grain and grain boundary are evident in the end products, and all the samples exhibit similar grain structure. It is clear from the photomicrograph that the particles are well separated, which could explain the agglomeration process that occurred during sample preparation.

To explore the effect of ion substitution in different positions, temperature dependence of magnetization of $YCrO_3$, $Y_{0.9}Ce_{0.1}CrO_3$ and $YCr_{0.9}Fe_{0.1}O_3$ measured in ZFC and FC mode with an applied magnetic field of 0.01 T is shown in Fig. 3. In all the samples, when the temperature is above 145 K, the magnetization decreases linearly with the increase of temperature, which indicating a paramagnetic behavior (PM). Magnetic phase transition occurred in the sample near 145 K. The magnetization curves of ZFC and FC modes show different behaviors at low temperature, that is, the magnetization curves have irreversibility, indicating that there is competition between different magnetic ordered. As shown in Fig. 3(a), in the $YCrO_3$ sample, there is a transition from paramagnetic to antiferromagnetic with decreasing temperature. The phase transition Neel temperature (T_N) is 145 K (T_N, defined as the first inflection point from high temperature to low temperature in the FC curve). For the doped samples, the T_N of $Y_{0.9}Ce_{0.1}CrO_3$ and $YCr_{0.9}Fe_{0.1}O_3$ are 145 K and 147 K, respectively. When some Y^{3+} ions are replaced by Ce^{3+}, the antiferromagnetic exchange interaction remains unchanged, which is because the antiferromagnetic order in the system originates from the exchange interaction of Cr-O-Cr. However, when Cr^{3+} ions are replaced by Fe^{3+}, the antiferromagnetic interaction is enhanced, and there are Cr-O-Cr and Fe-O-Cr antiferromagnetic exchange interactions in the system.

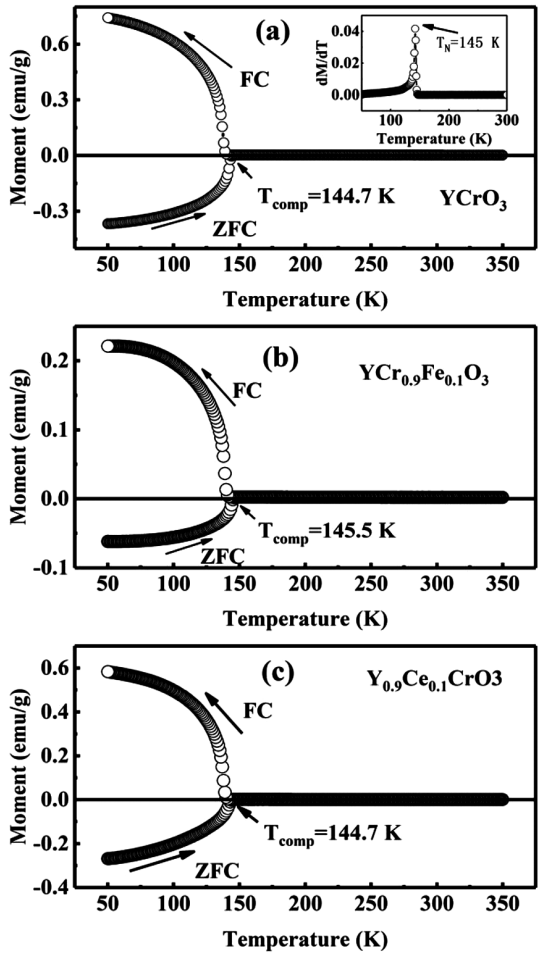

Fig. 3 — Temperature dependence of magnetization measured with 0.01 T magnetic field. The inset of (a) shows the differential of magnetization with respect to temperature, and the arrow indicates the magnetic transformation temperature T_N = 145K.

In the process of ZFC curve measurement, negative magnetization occurred in all samples. The compensation temperature of $YCrO_3$ and $Y_{0.9}Ce_{0.1}CrO_3$ is T_{comp}= 144.7 K, below which the magnetization is negative. However, the compensation temperature of the iron-doped samples is T_{comp}= 145.5 K, and the increase of the compensation temperature of $YCr_{0.9}Fe_{0.1}O_3$ is related to the change of magnetic coupling interaction between Fe^{3+} and Cr^{3+} caused by iron-doped. A similar magnetic behavior induced by Fe doping in has also been reported by Mao *et al.*[32]. The negative magnetization behavior below the compensation temperature can be attributed to the antiparallel magnetic coupling interaction between Fe-O-Fe /Cr and Cr-O-Fe/Cr, which results from the competition between single-ion magnetic anisotropy and antisymmetric DM interactions[32]. In the FC curve, the magnetization of $YCrO_3$ increased rapidly around 145 K, then gradually increased with the decrease of temperature, reaching saturation at 0.7 emu/g, indicating that the sample was ferromagnetic at low temperature. Due to the DM exchange between adjacent Cr^{3+} ions, Cr^{3+} ions are arranged in an antiferromagnetic array with inclination Angle. Therefore, the system generates ferromagnetism near the phase transition temperature, resulting in a sharp increase in the FC curve near the T_N. The Ce^{3+} ion-doped samples did not change the T_N and T_{comp} of the system, and the magnetization of the low temperature region did not change significantly. This may be because the interaction between Ce-Cr ions is similar to the interaction between Y-Cr ions, and the doping concentration is low, so the doping of Ce^{3+} ions have

little effect on the magnetic properties of the system. Cao *et al.*[33] reported the magnetic compensation of $CeCrO_3$ near 133 K, which was attributed to the antiparallel coupling between Ce^{3+} and Cr^{3+} moments. Thus, the magnetic curve of the system directly reflects the influence of the interaction between Cr^{3+} ions on its magnetism. In the Fig. 3(b), the intensity of ZFC and FC magnetization curves decreased significantly in the low temperature region, which is due to the enhanced antiferromagnetic interaction after Cr^{3+} was replaced by Fe^{3+}.

Figure 4 shows the isothermal hysteresis loops of samples (a) $YCrO_3$, (b) $YCr_{0.9}Fe_{0.1}O_3$ and (c) $Y_{0.9}Ce_{0.1}CrO_3$ at 50 K and 200 K. The magnetization curves of $YCrO_3$ and the doped samples are linear, indicating that the system is in paramagnetic state, which is consistent

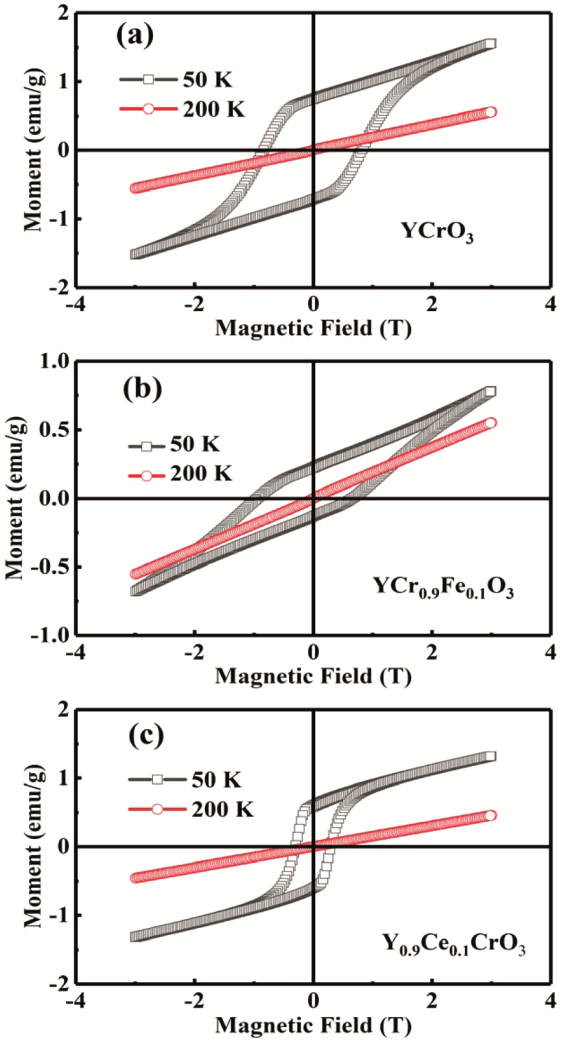

Fig. 4 — Magnetic field dependence of magnetization of (a)$YCrO_3$, (b) $YCr_{0.9}Fe_{0.1}O_3$ and (c) $Y_{0.9}Ce_{0.1}CrO_3$ at temperatures of 50 K and 200 K.

with the results of magnetothermal curves (The results show that the system is in paramagnetic state when T > 145 K). At 50 K temperature, the hysteresis loop of the sample is nonlinear and unsaturated with small hysteresis phenomena in the low field range, indicating that the system has weak ferromagnetism as well as antiferromagnetism. The hysteresis loops have different shapes when the samples are doped with different ions at 50 K. The hysteresis loops of $YCrO_3$ samples are full and close symmetrically, showing obvious ferromagnetism. When the magnetic field is greater than 1.5 T, there is no trend of magnetization saturation and it increases linearly, indicating that the system has antiferromagnetism. The unsaturated magnetization curve shows that the $YCrO_3$ system has both antiferromagnetism and ferromagnetism, and the co-existence of the two components is consistent with the weak ferromagnetism result caused by the canted antiferromagnetism spin of Cr^{3+} ions, which well accord with the published literatures[34]. As shown in Fig. 4(c) the variation trend of hysteresis loops of Ce^{3+} ion-doped samples is consistent with that of $YCrO_3$ samples and the magnetization does not change much. However, the coercivity of the hysteresis loop of $Y_{0.9}Ce_{0.1}CrO_3$ decreased obviously (Coercivity is defined as that, after saturation of magnetization, the magnetization does not retreat to zero when the external magnetic field back to zero. Only in the opposite direction of the original magnetic field plus a certain size of the magnetic field can make the magnetization back to zero, the magnetic field is called coercivity field, also known as coercivity.). The coercivity is strongly influenced by the grain size change. The decreased coercivity of the hysteresis loop of $Y_{0.9}Ce_{0.1}CrO_3$ may be caused by the fact that the ion radius of Ce^{3+} is larger than that of Y^{3+}. A similar result was observed in $La_{1-x}Ce_xCrO_3$[35]. The hysteresis loops of Fe^{3+} ion-doped samples are long and flat, which is different from the magnetization curves of $YCrO_3$ and $Y_{0.9}Ce_{0.1}CrO_3$. The magnetization curves of $YCr_{0.9}Fe_{0.1}O_3$ in both the low and high fields show a linear increase, and the magnetization intensity decreases significantly, as shown in Fig. 4(b). This indicates that the antiferromagnetism is prominent in the $YCr_{0.9}Fe_{0.1}O_3$ system, which is related to the anti-ferromagnetic exchange interaction between Fe^{3+} ions and Cr^{3+} ions. The doping of Fe^{3+} ions did not change the coercive force of the system.

3 Conclusions

The $YCrO_3$ and doped ceramic samples with orthogonal structure are successfully synthesized, and

the space group of the samples is Pnma. The magnetic properties of the system are systematically studied. The Cr^{3+} ions are canted antiferromagnetic in order near the magnetic phase transition temperature of 145 K, and the antiferromagnetic and ferromagnetic states coexisted in the system under low field and temperature. The negative magnetization induced by temperature is observed in $YCrO_3$, $Y_{0.9}Ce_{0.1}CrO_3$ and $YCr_{0.9}Fe_{0.1}O_3$. The magnetothermal properties of the system don't change when the Ce^{3+} ion doping at Y position, while the compensation temperature increased and the magnetization of the system reduced significantly when the Fe^{3+} ion doping at Cr^{3+} position. This is because the magnetism of $YCrO_3$ system mainly comes from the exchange coupling interaction between Cr ions, and the doping of Fe ions enhances the antiferromagnetism of the system. The experimental results provide a good experimental material for the possible application of rare-earth chromium oxide $YCrO_3$ in magnetic devices and the understanding of the physical mechanism in the system.

Acknowledgement

This work is supported by Henan College Key Research Project (Nos. 19B140001, 20A140002), Anyang Normal University College Student Innovation Fund (Nos. ASCX/2019-Z045, X2020104790108) and National Natural Science Foundation of China (No. 11747014).

References

1 White R L, *J Appl Phys*, 40 (1969) 1061.
2 Zhong W, Chen W, Ding W P, Zhang N, Hu A, Du Y W & Yan Q J, *J Magn Magn Mater*, 195 (1999) 112.
3 Vijayanandhini K, Simon C, Pralong V, Breard Y, Caignaert V, Raveau B, Mandal P, Sundaresan A & Rao C N R, *J Phys : Conden Matter*, 21 (2009) 486002.
4 Nair V G, Pal L, Subramanian V & Santhosh P N, *J Appl Phys*, 115 (2014) 17D728.
5 Su Y L, Zhang J C, Feng Z J, Li Z J, Shen Y & Cao S X, *J Rare Earths*, 29 (2011) 1060.
6 Bora T & Ravi S, *J Appl Phys*, 114 (2013) 033906.
7 Shi L R, Xia Z C, Huang S, Xiao G L, Jin Z, Wei M, Chen B R, Shang C, Cheng H & Ouyang Z w, *Ceram Int*, 42 (2016) 10808.
8 Shi L R, Wei C X & Xia Z C, *J Alloy Comp*, 698 (2017) 626.
9 Sharma Y, Sahoo S, Perez W, Mukherjee S, Gupta R, Garg A, Chatterjee R & Katiyar R S, *J Appl Phys*, 115 (2014) 183907.
10 Zvezdin A K & Mukhin A A, *JETP letters*, 88 (2008) 505.
11 Yoshii K, *J Solid State Chem*, 159 (2001) 204.
12 Yoshii K, Nakamura A, Ishii Y & Morii Y, *J Solid State Chem*, 162 (2001) 84.
13 Mandal P, Serrao C R, Suard E, Caignaert V, Sundaresan A & Rao C N R, *J Solid State Chem*, 197 (2013) 408.
14 Mandal P, Sundaresan A, Rao C N R, Iyo A, Shirage P M, Tanaka Y, Simon C, Pralong V, Lebedev O I, Caignaert V & Raveau B, *Phys Rev B*, 82 (2010) 100416.
15 Azad A K, Mellergård A, Eriksson S G, Ivanov S A, Yunus S M, Lindberg F, Svensson G & Mathieu R, *Mater Res Bull*, 40 (2005) 1633.
16 Belik A A, Abakumov A M & Tsirlin A A, *Chem Mater* 23 (2011) 4505.
17 Dasari N, Mandal P, Sundaresan A & Vidhyadhiraja N S, EPL (*Europhys Lett*), 99 (2012) 17008.
18 Sinha R, Basu S & Meikap A K, *Mater Res Bull*, 97 (2018) 578.
19 Sinha R, Kundu S, Basu S & Meikap A K, *Solid State Sci*, 60 (2016) 75.
20 Kumar S, Coondoo I, Rao A, Lu B, Kuo Y, Kholkin A L & Panwar N, *Physica B* 510 (2017) 104.
21 Duran A, Verdin E, Conde A & Escamilla R, *J Magn Magn Mater* 453 (2018) 36.
22 Li C L, Huang S, Li X X, Zhu C M, Zerihun G, Yin C Y, Lu C L & Yuan S L, *J Magn Magn Mater*, 432 (2017) 77.
23 Sinha R, Basu S & Meikap A K, *Physica E*, 113 (2019) 194.
24 Chakraborty P, Dey S & Basu S, *Physica B: Condensed Matter* 601 (2021) 412477.
25 Chakraborty P, Rana D K & Basu S, *Bull Mater Sci*, 44 (2021) 133.
26 Chakraborty P & Basu S, *Mater Chem Phys*, 259 (2021) 124053.
27 Duran A, Verdin E, Conde A & Escamilla R, *J Magn Magn Mater*, 453 (2018) 36.
28 Hashimi A G, Ould M L, Zaari H, Youssef A Ben & Kenz A, *J Supercond Nov Magnet*, 30 (2017) 483.
29 Wang H L, Liu X Z, Sun K, Ma X B, Guo H, Bobrikov I A, Sui Y, Liu Q Y, Xia Y H, Chen X P, Li Z Y, Hao L J, Liu Y T & Chen D F, *J Magn Magn Mater*, 535 (2021) 168022.
30 Tiwari1 S, Saleem1 M, Mishra1 A & Varshney D, *J Supercond Nov Magnet*, 32 (2019) 2521.
31 Sonia M M L, Anand S, Maria V, Janifer M A, Pauline S & Manikandan A, *J Magn Magn Mater* 466 (2018) 238.
32 Mao J, Sui Y, Zhang X, Su Y T, Wang X J, Liu Z G, Wang Y, Zhu R B, Liu W F & Tang J K, *Appl Phys Lett*, 98 (2011) 192510.
33 Cao Y M, Cao S X, Ren W, Feng Z J, Yuan S J, Kang B J, Lu B & Zhang J C, *Appl Phys Lett*, 104 (2014) 232405.
34 Serrao C R, Kundu Asish K, Krupanidhi S B, Waghmare U V & Rao C N R, *Phys Rev B* 72 (2005) 220101.
35 Shukla R, Manjanna J, Bera A K, Yusuf S M & Tyagi A K, *Inorg Chem*, 48 (2009) 11691.